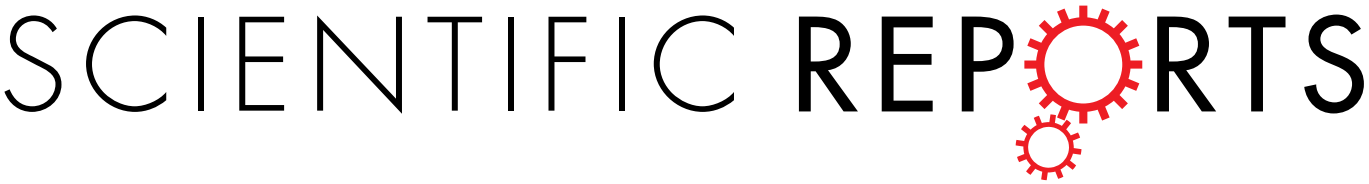

OPEN

Comparison of bone texture between normal individuals and patients with Kashin-Beck disease from plain radiographs in knee

Received: 13 March 2018
Accepted: 7 November 2018
Published online: 30 November 2018

Wenrong Li[1,2], Jukka Hirvasniemi[3], Xiong Guo[2], Simo Saarakkala[4,5,6], Mikko J. Lammi[2,7] & Chengjuan Qu[7]

To compare tibial bone texture between Kashin-Beck disease (KBD) patients and normal individuals from plain radiographs using an advanced image analysis. Plain knee radiographs were obtained from KBD patients (n = 49) and age-matched healthy controls (n = 98). KBD were graded with diagnostic criteria WS/T 207-2010. The textural values related to bone structure from medial and lateral tibial subchondral and trabecular bones were evaluated using entropy of Laplacian-based image (E_{Lap}), entropy of local binary patterns (E_{LBP}), homogeneity indices (HI) of local angles (HI_{Mean}, HI_{Perp} and HI_{Paral}), and fractal dimensions from horizontal (FD_{Hor}) and vertical (FD_{Ver}) structures. KBD patients were shorter in height and lighter in weight, and their tibial width was wider than controls. Anatomical angle of KBD patients showed more genu valgus. Total KBD patients and subgroups had higher E_{Lap}, HI_{Mean}, HI_{Perp} and HI_{Paral} in detected tibial subchondral and trabecular bones than controls, except E_{Lap} in lateral subchondral bone. E_{LBP}, FD_{Hor} and FD_{Ver} from the detected tibial bone in KBD patients and subgroups were lower than controls, except FD_{Ver} in lateral trabecular bone. Our results indicate that micro-scale in bone texture in KBD-affected knees can be quantitatively examined from plain radiographs using an advanced image analysis.

Kashin-Beck disease (KBD) is a chronic endemic and degenerative form of osteoarthritis (OA), which is distributed primarily in agricultural regions of southeastern Siberia, northern Korea, and China[1–3]. It causes pain, discomfort and disability to work already at young age. The incidence of KBD has remarkably declined over the last decades, but the disease is still readily observable in the endemic areas, such as Linyou and Yongshou counties at Shaanxi province in China. Despite increasing research on KBD, its etiology remains still unclear.

The KBD's clinical symptoms are pain, enlargement, morning stiffness, dysfunction, short fingers/limbs and even deformation in the affected joints, which lead to limitations in movements (Fig. 1). Conventional low-cost radiography using a simple and fast two-dimensional (2D) projection has proved to be the best way to diagnose KBD along with patients' history and symptoms evaluated according to diagnostic criteria WS/T 207–2010 (Supplemental Table 1)[1,4]. The characteristic features of KBD in plain radiography are blurred, interrupted and irregular marginal sclerosis in epiphysis and/or metaphysis[5,6]. Macro-scale changes of bone tissues can be easily observed from plain radiographs which provide very useful morphological information of the disease-affected bone density and structure. However, these changes are difficult to visually evaluate from plain radiographs due to flat image and overlapping anatomical structures, as compared to three-dimensional (3D) imaging.

[1]Department of Medical Imaging, The First Affiliated Hospital of Xi'an Jiaotong University, 277 West Yanta Road, Xi'an Shaanxi, 710061, P. R. China. [2]School of Public Health, Xi'an Jiaotong University Health Science Center, Xi'an, P. R. China. [3]Center for Machine Vision and Signal Analysis, Faculty of Information Technology and Electrical Engineering, University of Oulu, Oulu, Finland. [4]Research Unit of Medical Imaging, Physics and Technology, Faculty of Medicine, University of Oulu, Oulu, Finland. [5]Medical Research Center Oulu, Oulu University Hospital and University of Oulu, Oulu, Finland. [6]Department of Diagnostic Radiology, Oulu University Hospital, Oulu, Finland. [7]Department of Integrative Molecular Biology, Umeå University, 90187, Umeå, Sweden. Correspondence and requests for materials should be addressed to C.Q. (email: chengjuan.qu@gmail.com) or X.G. (email: guox@mail.xjtu.edu.cn)

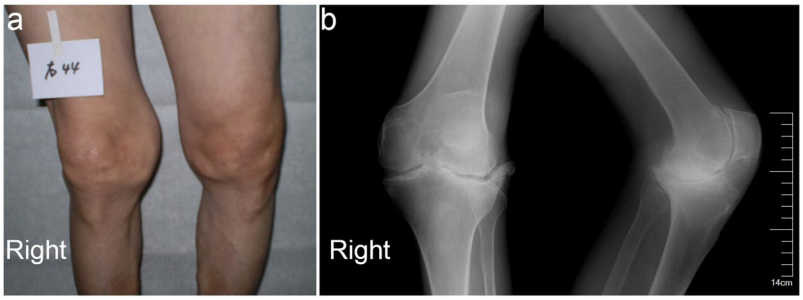

Figure 1. Clinical (**a**) and radiological (**b**) findings in a 55-year old female with KBD in right knee joint.

Parameter		Mean ± SD					
Subjects (KBD grades)		Control (0)	KBD total (KBD)	KBD grade 1 (1)	KBD grade 2 (2)	KBD grade 3 (3)	Statistical significance
Age (years)		51.2 ± 8.6	52.1 ± 10.7	51.7 ± 12.2	54.1 ± 8.2	48.4 ± 11.3	none
Height (cm)		161.0 ± 6.8	155.5 ± 9.8	158.0 ± 9.0	154.2 ± 7.6	150.4 ± 15.1	0-KBD**, 0–2*, 0–3*
Weight (kg)		59.0 ± 8.3	52.7 ± 9.4	54.7 ± 10.3	51.8 ± 8.5	48.0 ± 7.0	0-KBD**, 0–1*, 0–2**, 0–3**
Body mass index (kg/m^2)		22.7 ± 2.6	21.7 ± 2.7	21.8 ± 2.9	21.7 ± 2.3	21.3 ± 2.8	0-KBD*
Gender	Female	70	32	17	11	4	
	Male	28	17	7	7	3	

Table 1. Basic information of the subjects used in the present study. Normal control subjects, n = 98; total KBD patients, n = 49; KBD grade 1, n = 24, KBD grade 2, n = 18 and KBD grade 3, n = 7. SD: standard deviation; KBD: Kashin-Beck disease; **stands for p value is equal or less than 0.001, *represents that p value is less than 0.05.

Radiologists often diagnose bone disease using trabecular bone microarchitecture. However, the anatomy and mechanical properties of trabecular bone are not easy to observe precisely due to the shape and distribution of trabecular networks. Trabecular bone microstructure from 2D radiographs and local binary patterns (LBP) -based methods[7] for plain radiographs have been used for OA studies. It has been reported that bone density or/and structure, evaluated from 2D radiographs of different bones using these techniques, are strongly correlated with true 3D microstructure in normal and diseased human individuals[8–13]. Bone texture in normal and osteoarthritic knees has been quantitatively evaluated from 2D radiographs using Laplacian-based and LBP-based images[7,10,14], which showed that bone structure-related parameters had significant differences between different OA grades, and between healthy control and OA groups[7,15].

To our knowledge, there are no any studies on bone texture analysis from 2D radiography in KBD patients yet. Therefore, we aimed to quantify whether the differences in bone structure between healthy individuals and KBD patients, and within various grades of KBD patients can be revealed from 2D radiographs using bone texture analysis methods. We hypothesized that bone structure-related texture parameters measured with Laplacian-based, LBP-based and FSA-based methods are different between healthy individuals and KBD patients or their subgroups.

Results

Height, weight and body mass index (BMI) were smaller in total KBD patients than the age-matched controls, as did the height in KBD grades 2 and 3, as well weight in all KBD sub-groups (Table 1, Supplemental Table 1). Width of the tibia in total KBD patients and KBD grades 2 and 3 was larger than the controls, while anatomical angle in KBD grade 1 and 3 was larger than the controls, showing genu valgus (Table 2). MedJSW in KBD grade 3 was lower than the controls and KBD grade 1, as well as it was also lower in KBD grade 2 than grade 1 (Table 2).

Statistically significant differences were observed in bone texture parameters. In medial subchondral bone, E_{Lap} in total KBD patients and all KBD subgroups was higher than the controls, as well as it was lower in KBD grades 2 and 3 compared to grade 1 (Fig. 2a, Table 3). HI_{Mean}, HI_{Perp} and HI_{Paral} were higher in total KBD patients, as well in various KBD subgroups than the controls (Fig. 3a,c,e, Table 3). Furthermore, HI_{Mean} and HI_{Paral} were also higher in KBD grades 2 and 3 than grade 1 (Table 3). However, E_{LBP}, FD_{Hor} and FD_{Ver} were lower in total KBD patients and various KBD subgroups than the controls (Figs 2c, and 4a,c, Table 3).

In lateral subchondral bone, E_{Lap} was higher in various KBD subgroups than the control, as well as it was higher in KBD grade 1 than grade 2, but no significant difference was observed on E_{Lap} between controls and total KBD patients (Fig. 2a, Table 3). HI_{Mean}, HI_{Perp} and HI_{Paral} were higher in total KBD patients as well in various KBD subgroups than the controls (Fig. 3a,c,e, Table 3). E_{LBP}, FD_{Hor} and FD_{Ver} were lower in total KBD patients as well as in various KBD subgroups than the controls (Figs 2c and 4a,c, Table 3). Moreover, E_{LBP} in KBD grade 2 was lower than grade 1 (Table 3).

Parameter	Mean ± SD					
Subjects (KBD grades)	Control (0)	KBD total (KBD)	KBD grade 1 (1)	KBD grade 2 (2)	KBD grade 3 (3)	Statistical significance
medJSW	4.22 ± 0.9	3.96 ± 1.2	4.38 ± 0.8	3.71 ± 1.3	3.15 ± 1.3	0–3*, 1–2*, 1–3*
latJSW	4.03 ± 1.0	4.15 ± 1.8	4.24 ± 1.8	4.19 ± 2.1	3.76 ± 0.8	none
Tibia width	73.18 ± 5.1	77.09 ± 7.6	75.17 ± 7.0	79.80 ± 8.2	76.69 ± 6.7	0-KBD**, 0–2**, 0–3*
Anatomical angel, genu valgus	182.11 ± 2.9	183.60 ± 7.0	183.78 ± 4.1	182.92 ± 10.5	184.71 ± 3.1	0–1*, 0–3*
	−2.11 ± 2.9	−3.60 ± 7.0	−3.78 ± 4.1	−2.92 ± 10.5	−4.71 ± 3.1	0–1*, 0–3*

Table 2. Mean values (±SD) of medJSW, latJSW, tibia width and anatomical angle of the knees from the subjects. Normal control subjects, n = 98; total KBD patients, n = 49; KBD grade 1, n = 24, KBD grade 2, n = 18 and KBD grade 3, n = 7. SD: standard deviation; KBD: Kashin-Beck disease; medJSW: minimum joint space width measured from 75% medial compartment; latJSW: minimum joint space width measured from 75% lateral compartment; Genu varus/valgus were calculated with the equation: 180° - anatomical angle; **stands for p value is equal or less than 0.001, *represents that p value is less than 0.05.

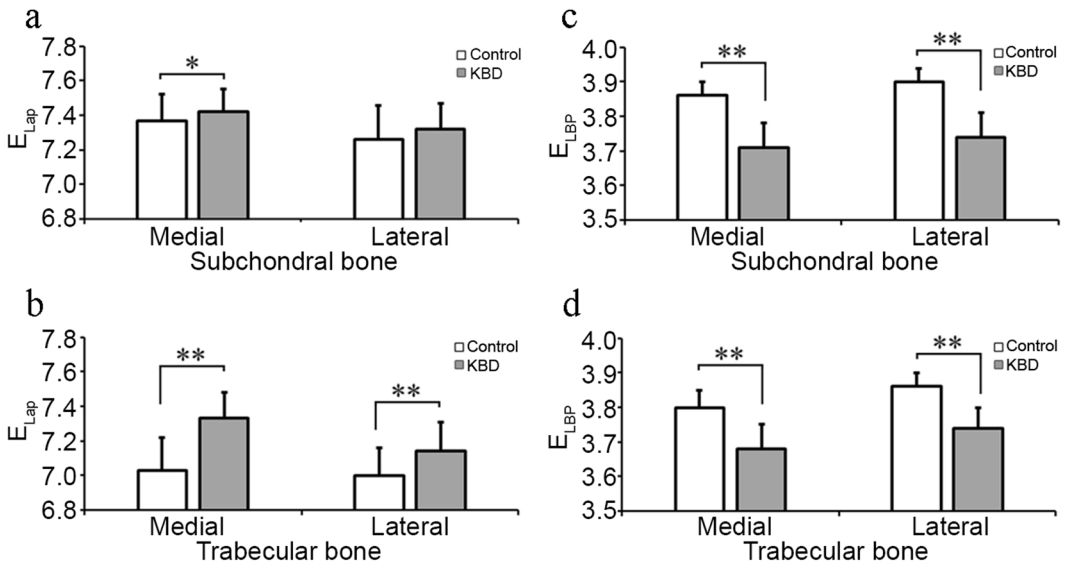

Figure 2 . Representative mean ± SD and statistical significance of bone structural parameters, entropy of laplacian-based image (E_{lap}) and local binary patterns (E_{LBP}) measured from medial and lateral subchondral and trabecular bone between control healthy individuals ($n = 98$) and Kashin-Beck disease (KBD, $n = 49$) patients. *Stands for $P < 0.05$, **Stands for $P \leq 0.001$.

In medial trabecular bone, E_{Lap}, HI_{Mean}, HI_{Perp} and HI_{Paral} were higher in total KBD patients and various KBD subgroups than the controls (Figs 2b and 3b,d,f, Table 4), as well as HI_{Mean} and HI_{Perp} were higher in KBD grades 2 or 3 than grade 1 (Table 4). E_{LBP}, FD_{Hor} and FD_{Ver} in total KBD patients and various KBD subgroups were lower than the controls (Figs 2d, and 4b,d, Table 4). Furthermore, E_{LBP} was lower in KBD grade 2 than grade 1 (Table 4), and FD_{Ver} was lower in KBD grades 2 and 3 than the controls (Table 4).

In lateral trabecular bone, E_{Lap}, HI_{Mean}, HI_{Perp} and HI_{Paral} were higher in total KBD patients and various KBD subgroups than the age-matched controls, besides HI_{Mean} and HI_{Paral} were higher in KBD grades 2 and 3 than grade 1, and HI_{Perp} was higher in KBD grade 2 than grade 1 (Figs 2b, and 3b,d,f, Table 4). However, E_{LBP} and FD_{Hor} in total KBD patients and various KBD subgroups were lower than the controls, as well as E_{LBP} was lower too in KBD grade 2 and 3 than grade 1 (Figs 2d, and 4b, Table 4). However, no significant difference could be seen on FD_{Ver} between KBD groups and the controls (Table 4).

Discussion

Our results revealed that the diseased subjects had lower height, weight, anatomical femur-tibia angle and medJSW, but wider tibia, confirming that the patients investigated here suffered from KBD[1]. The most interesting findings in this study are that the bone structure measured from medial and lateral tibial subchondral and trabecular bones from 2D radiographs showed statistical differences in KBD patients and/or their subgroups when compared to controls, which shows in following parameters: E_{Lap}, E_{LBP}, HIs, and FDs. Interestingly, the changes of the bone texture parameters in KBD are mostly opposite to OA patients when compared to controls, suggesting that micro-structural changes in bone are not identical to OA (Supplemental Table 2).

E_{Lap} is used to examine randomness of the pixel in an image, whereas E_{LBP} measures randomness of local binary patterns[7,15,16]. When E_{Lap} is equal to zero, the image is perfectly flat and pixel intensities are identical within

Side of joint	Parameter	Control (0)	KBD total (KBD)	KBD grade 1 (1)	KBD grade 2 (2)	KBD grade 3 (3)	Statistical significance
Medial subchondral bone	E_{Lap}	7.37 ± 0.15	7.42 ± 0.13	7.46 ± 0.12	7.37 ± 0.14	7.44 ± 0.06	0–KBD*, 0–1*, 0–2*, 0–3*, 1–2*, 1–3*
	E_{LBP}	3.86 ± 0.04	3.71 ± 0.07	3.72 ± 0.08	3.70 ± 0.06	3.70 ± 0.06	0–KBD**, 0–1**, 0–2**, 0–3**
	HI_{Mean}	0.67 ± 0.01	0.69 ± 0.01	0.69 ± 0.01	0.70 ± 0.01	0.71 ± 0.02	0–KBD**, 0–1**, 0–2**, 0–3**, 1–2*, 1–3*
	HI_{Perp}	0.66 ± 0.01	0.68 ± 0.01	0.68 ± 0.01	0.69 ± 0.01	0.69 ± 0.02	0-KBD**, 0–1**, 0–2**, 0–3**
	HI_{Paral}	0.68 ± 0.01	0.70 ± 0.02	0.69 ± 0.01	0.71 ± 0.01	0.71 ± 0.02	0–KBD**, 0–1**, 0–2**, 0–3**, 1–2*, 1–3*
	FD_{Hor}	2.50 ± 0.09	2.35 ± 0.15	2.39 ± 0.16	2.33 ± 0.14	2.30 ± 0.12	0-KBD**, 0–1**, 0–2**, 0–3**
	FD_{Ver}	2.78 ± 0.06	2.72 ± 0.12	2.74 ± 0.09	2.69 ± 0.12	2.71 ± 0.17	0–KBD**, 0–1*, 0–2**, 0–3*
Lateral subchondral bone	E_{Lap}	7.26 ± 0.20	7.32 ± 0.15	7.37 ± 0.10	7.26 ± 0.16	7.33 ± 0.20	0–1*, 0–2*, 0–3*, 1–2*
	E_{LBP}	3.90 ± 0.04	3.74 ± 0.07	3.77 ± 0.07	3.72 ± 0.08	3.74 ± 0.07	0–KBD**, 0–1**, 0–2**, 0–3**, 1–2*
	HI_{Mean}	0.67 ± 0.01	0.69 ± 0.02	0.68 ± 0.01	0.69 ± 0.02	0.69 ± 0.02	0–KBD**, 0–1**, 0–2**, 0–3**
	HI_{Perp}	0.66 ± 0.01	0.68 ± 0.02	0.67 ± 0.02	0.68 ± 0.01	0.68 ± 0.01	0–KBD**, 0–1**, 0–2**, 0–3**
	HI_{Paral}	0.68 ± 0.01	0.69 ± 0.02	0.69 ± 0.01	0.70 ± 0.02	0.70 ± 0.02	0–KBD**, 0–1**, 0–2** 0–3**
	FD_{Hor}	2.60 ± 0.10	2.43 ± 0.13	2.46 ± 0.13	2.43 ± 0.14	2.39 ± 0.06	0–KBD**, 0–1**, 0–2**, 0–3**
	FD_{Ver}	2.82 ± 0.06	2.75 ± 0.11	2.77 ± 0.10	2.73 ± 0.12	2.72 ± 0.11	0–KBD**, 0–1*, 0–2**, 0–3**

Table 3. Mean values (±SD) of the measurement related to the bone structural parameters in control (n = 98) and KBD (n = 49) subjects from medial and lateral subchondral bone plate in tibia. SD: standard deviation; KBD: Kashin-Beck disease; E_{lap}: entropy of Laplacian-based image; E_{LBP}: entropy of local binary patterns; HI_{mean}: homogeneity index for orientation of local patterns; HI_{perp}; HI perpendicularly to the bone trabeculae; HI_{paral}: HI parallel to the bone trabeculae; FD_{hor}: fractal dimension of horizontal structures; FD_{ver}: fractal dimension of vertical structures. no: no statistical significance. **Stands for p value is equal or less than 0.001, *represents that p value is less than 0.05.

image. Lower E_{Lap} indicates lower variation in the image pixel intensities. However, when E_{LBP} is equal to zero, it means that there is only one pattern occurring in the analyzed image. Lower E_{LBP} value indicates lower number of the grouped LBPs in the analyzed image. In this study, inverse relationship between E_{Lap} and E_{LBP} was observed in KBD similarly to OA, although in an opposite direction. Therefore, the increased E_{Lap} and decreased E_{LBP} indicates that KBD have more variation in grayscale values in the detected bones than controls, but less variation in different LBPs in the image. Since our studied subjects are mainly mild and moderate KBD cases, the less disorganized different patterns in KBD may act as remodeling of the bone structure and keep the balance for local disoriented pattern before developing to OA, even though the increased E_{LBP} noticed in advanced OA[7]. In KBD, the paramount histopathologic changes are chondrogenesis, secondary repair and tissue remodeling, and they may happen separately or even simultaneously[6].

The higher HI, the more connected trabecular fibers are in an image. The more similar orientation in the adjacent patterns, the closer to one the value of HI will be. Thus, the variation in various directions of local patterns would be low in that case. Our results with higher HI_{Mean}, HI_{Perp} and HI_{Paral} in KBD, but less than one, indicated that the orientation of neighbouring patterns is more similar to the local ones, and more connected to the main trabecular fibers, as the trabeculae are more vertically aligned than horizontally. This is further confirmed with the increased E_{lap} and the decreased E_{LBP} in this study, which showed better connectivity of bone structure and the adjacent patterns differed less from each other in KBD, but opposite to advanced OA (Supplemental Table 2)[7,15].

FDs were calculated locally in vertical and horizontal directions with FSA method, which provides the most precise characteristics of roughness of trabecular bone texture[17,18]. FSA has been suggested as a potentially efficient mean to predict OA progression and help on the treatment and research[19]. A significantly lower FD_{Hor} and FD_{ver} in KBD in this study indicated the thickening of the trabeculae in horizontal and vertical directions in both sides of the tibia, and may cause trabecular sclerosis similarly to the findings observed in KBD hand radiographs[1,6]. A loss of bone and bone structure from both sides appears obvious, although no significant changes observed in FD_{ver} in lateral trabecular bone. These are consistent with previous studies on OA knees with Kellgren & Lawrence (KL) grade 2 or worse, which showed significantly lower FDs in OA knees than controls (Supplemental Table 2)[20,21]. However, this finding is inconsistent with previous results of lower E_{Lap} and HIs, and higher E_{LBP} and FDs on KL grade 2 or worse OA[15]. One explanation for the contradicting results is that the KBD recruited for this study were mostly at mild and moderate disease stage. Moreover, the reactive bone proliferation and disturbance of bone formation are the secondary changes in KBD besides the primary changes on cartilage[6]. Another explanation is that KBD patients had lower BMI whereas OA typically have higher BMI than controls.

This study contains certain limitations that should be addressed. First, the imaging settings were not completely consistent for the subjects, which might have affected image quality and bone texture parameters. To avoid this factor, same equipment, imaging parameters and calibration object in the image should be used in future studies. To overcome this issue in this study, the images were resampled to a same pixel size, median filtered, and grayscale value range was expanded to full dynamic range. Texture parameter are robust to change in magnitude of grayscale values in image. Second, due to different diagnostic criteria used for KBD and OA, the comparison of their bone texture parameters showed a difference. Finally, the imaging findings, such as cysts and sclerosis, can also affect bone texture. Therefore, it would be advantageous to use same radiographic criteria to diagnose KBD and OA in order to make effective comparison.

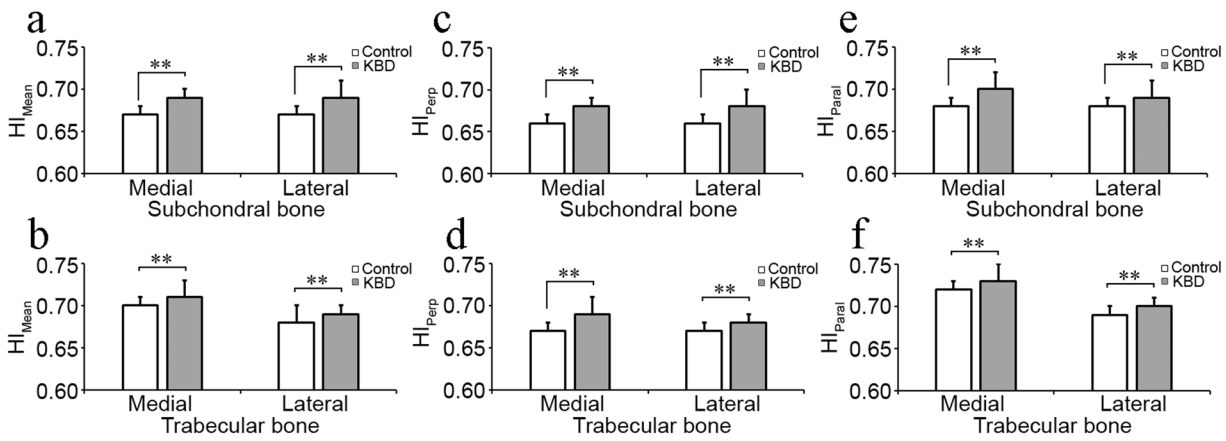

Figure 3. Representative mean ± SD and statistical significance of bone structural parameters, mean of homogeneity index (HI_{Mean}) and HI perpendicular (0°, HI_{Perp}) and parallel (90°, HI_{Paral}) to the trabecular main orientation, measured from medial and lateral subchondral and trabecular bone between control individuals ($n = 98$) and Kashin-Beck disease (KBD, $n = 49$). *Stands for $P < 0.05$, **Stands for $P \leq 0.001$.

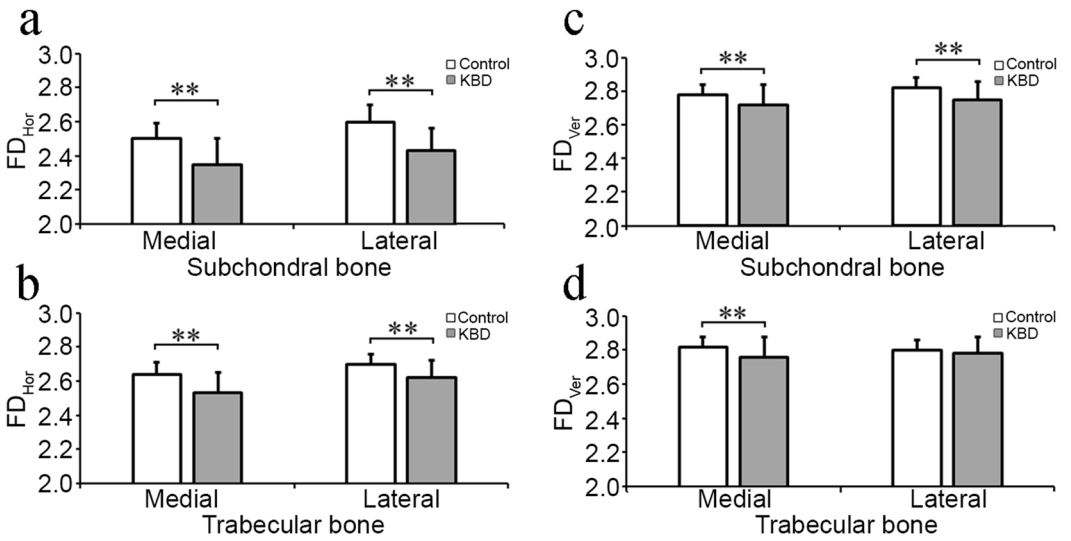

Figure 4. Representative mean ± SD and statistical significance of bone structural parameters, fractal dimension of horizontal (FD_{Hor}) and vertical structures (FD_{Ver}), measured from medial and lateral subchondral and trabecular bone between control individuals ($n = 98$) and Kashin-Beck disease (KBD, $n = 49$). *Stands for $P < 0.05$, **stands for $P \leq 0.001$.

Conclusion

The bone texture structure in KBD had clearly changed in subchondral and trabecular bone. The Laplacian-based, LBP-based, and FSA methods are powerful tools to quantify micro-scale changes of KBD in bone texture anisotropy, randomness and roughness. These analyses can be easily performed with a low-cost 2D digitalized high-resolution radiographs. The findings on micro-changes of anisotropy, connectivity and roughness underlying subchondral bone could play a key role in the initiation and progression of KBD knee joints. The incidence of KBD is high during age 5–15 years old, and hands are most frequently affected. Hand radiographs are usually the first choice to diagnose and classify KBD. The developed FSA methods have been successfully used to evaluate trabecular bone texture in OA knee and hand radiographs[22,23]. Therefore, our future work on hand bone texture analysis could provide wider knowledge for early stage diagnosis of KBD and young patients, and prevention and treatment.

Plain radiographs has been utilized as a general examination method in the diagnostic of KBD, which can provide very useful information on the morphological changes of the affected bone density and structure at macro-scale. Thus, it has been used as a first diagnostic tool in radiology for KBD. However, the microarchitecture changes in subchondral and trabecular bone in KBD or other bone disease are not easy to quantify reliably in the basic plain radiographs with visual evaluation. Therefore, the bone texture structure analysis with Laplacian-based, LBP-based and FSA methods would provide more quantitative data of the micro-scale changes

Side of joint	Parameter	Control (0)	KBD total (KBD)	KBD grade 1 (1)	KBD grade 2 (2)	KBD grade 3 (3)	Statistical significance
Medial trabecular bone	E_{Lap}	7.03 ± 0.19	7.33 ± 0.15	7.31 ± 0.16	7.35 ± 0.15	7.34 ± 0.18	0–KBD**, 0–1**, 0–2**, 0–3**
	E_{LBP}	3.80 ± 0.05	3.68 ± 0.07	3.70 ± 0.06	3.66 ± 0.07	3.68 ± 0.11	0–KBD**, 0–1**, 0–2**, 0–3**, 1–2*
	HI_{Mean}	0.70 ± 0.01	0.71 ± 0.02	0.71 ± 0.01	0.72 ± 0.01	0.71 ± 0.03	0–KBD**, 0–1**, 0–2**, 0–3**, 1–2*
	HI_{Perp}	0.67 ± 0.01	0.69 ± 0.02	0.69 ± 0.01	0.70 ± 0.01	0.69 ± 0.03	0–KBD**, 0–1**, 0–2**, 0–3**, 1–2*, 1–3*
	HI_{Paral}	0.72 ± 0.01	0.73 ± 0.02	0.72 ± 0.02	0.73 ± 0.01	0.73 ± 0.02	0–KBD**, 0–1*, 0–2**, 0–3**
	FD_{Hor}	2.64 ± 0.07	2.53 ± 0.12	2.56 ± 0.12	2.49 ± 0.11	2.51 ± 0.11	0 – KBD**, 0–1**, 0–2**, 0–3**
	FD_{Ver}	2.82 ± 0.06	2.76 ± 0.12	2.79 ± 0.08	2.71 ± 0.11	2.76 ± 0.21	0 – KBD**, 0–2**, 0–3**, 1–2*, 1–3*
Lateral trabecular bone	E_{Lap}	7.00 ± 0.16	7.14 ± 0.17	7.12 ± 0.18	7.15 ± 0.17	7.21 ± 0.15	0–KBD**, 0–1*, 0–2**, 0–3**
	E_{LBP}	3.86 ± 0.04	3.74 ± 0.06	3.76 ± 0.04	3.71 ± 0.05	3.72 ± 0.08	0–KBD**, 0–1**, 0–2**, 0–3**, 1–2**, 1–3*
	HI_{Mean}	0.68 ± 0.01	0.69 ± 0.01	0.69 ± 0.01	0.70 ± 0.01	0.69 ± 0.02	0–KBD**, 0–1*, 0–2**, 0–3**, 1–2*, 1–3*
	HI_{Perp}	0.67 ± 0.01	0.68 ± 0.01	0.68 ± 0.01	0.69 ± 0.01	0.68 ± 0.01	0–KBD**, 0–1**, 0–2**, 0–3**, 1–2*
	HI_{Paral}	0.69 ± 0.01	0.70 ± 0.01	0.70 ± 0.01	0.71 ± 0.01	0.71 ± 0.02	0–KBD**, 0–2**, 0–3**, 1–2*, 1–3*
	FD_{Hor}	2.70 ± 0.06	2.62 ± 0.10	2.64 ± 0.10	2.60 ± 0.10	2.58 ± 0.10	0–KBD**, 0–1**, 0–2**, 0–3**
	FD_{Ver}	2.80 ± 0.06	2.78 ± 0.10	2.80 ± 0.09	2.75 ± 0.09	2.78 ± 0.13	none

Table 4. Mean values (±SD) of the measurement related to the bone structural parameters in control (n = 98) and KBD (n = 49) subjects from medial and lateral trabecular bone in tibia. SD: standard deviation; KBD: Kashin-beck disease; E_{lap}: entropy of Laplacian-based image; E_{LBP}: entropy of local binary patterns; HI_{mean}: homogeneity index for orientation of local patterns; HI_{perp}; HI perpendicularly to the bone trabeculae; HI_{paral}: HI parallel to the bone trabeculae; FD_{hor}: fractal dimension of horizontal structures; FD_{ver}: fractal dimension of vertical structures. **Stands for p value is equal or less than 0.001, *represents that p value is less than 0.05.

of KBD patients in bone texture anisotropy, randomness and roughness, and may help in the clinical diagnostic of the disease at early stage.

Methods

Study materials. A total of 116 controls and 77 KBD patients were primarily recruited in the study. Of these, 18 controls and 28 KBD patients were excluded in the study due to the quality of the plain radiographs and/or the presence of osteophytes, which would affect the measurements. Thus, 98 controls and 49 KBD patients were included in the analysis of the present study. 98 healthy individuals (age: 51.2 ± 8.6; 28 male and 70 female) with 98 plain radiographs were randomly selected from non-endemic area, which was close to the endemic area, and had similar environment concerning geography, climate and life style as the endemic KBD area. 49 KBD patients (age: 52.1 ± 10.7; 17 male; 32 female) with 49 plain radiographs were selected from endemic disease areas. Written informed consent was obtained from all studied subjects and/or their legal guardians with permission to be used as their personal background information in the study. This study was reviewed and approved by "The first Affiliated Hospital of Xi´an Jiaotong University Ethics Committee", and the project implementation process was in line with the ethical principles.

Acquisition of plain radiographs and grading of knees. Right knees of control ($n = 98$) and 46 right and three left knees of KBD patients ($n = 49$) were imaged at posterior-anterior fixed–flexion position using digital radiographies with tube voltage: 55–65 kV, quantity of charge: 200 mA, exposure time: 12–20 ms and source-detector distance: 85 cm. The KBD patients were graded based on the diagnostic criteria of clinical appearance (http://www.moh.gov.cn/zwgkzt/s9500/201006/47920.shtml, Supplemental Table 1). For grading, value one means mild KBD, while three indicates severe KBD (Table 1). All the imaged knees were analyzed with a custom-made MATLAB software (v7.9.0; MathWorks Inc., Natick, MA, USA). In order to get reliable measured parameters, all images were rescaled to a pixel size of 150 µm adjusted to achieve a full dynamic range and converted to 8-bit before analyses.

Selection of regions of interest. As previous studies described[7,15], two ROIs (93 × 40 pixels) subchondral bone were placed in the center of medial and lateral condyle of tibia below cartilage-bone interface, and two other ROIs (93 × 93 pixels) for trabecular bone were closely placed below and parallel to the dense subchondral bone. The minimum medial (medJSW) and lateral joint space widths (latJSW) were also measured in the narrowest point of joint from both medial and lateral sides as previously described[7]. The width of tibia was measured from the corners of both sides of the bone. The anatomical angle was measured based on a gold standard criterion in a full limb radiograph, where mechanical-axis angle (180°) was used as reference standard, with angles <180° defined as genu varus, and angles >180° defined as genu valgus[24] (Fig. 5).

Analysis of bone texture. The structure of bone texture was analyzed using Laplacian-based, LBP-based[7,10,14–16], and FSA-based methods[10,18] after the radiographs were median-filtered (3 × 3 pixels) to eliminate the high frequency noise from the images.

Laplacian-based analysis. Laplacian-based method has been clearly shown to promote the appearance of bone trabeculae and quantitatively determine the variations in the grayscale values on Laplacian-based images[14]. As previous studies described in Laplacian-based analysis[7,14,15], the Laplacians were calculated in both vertically and

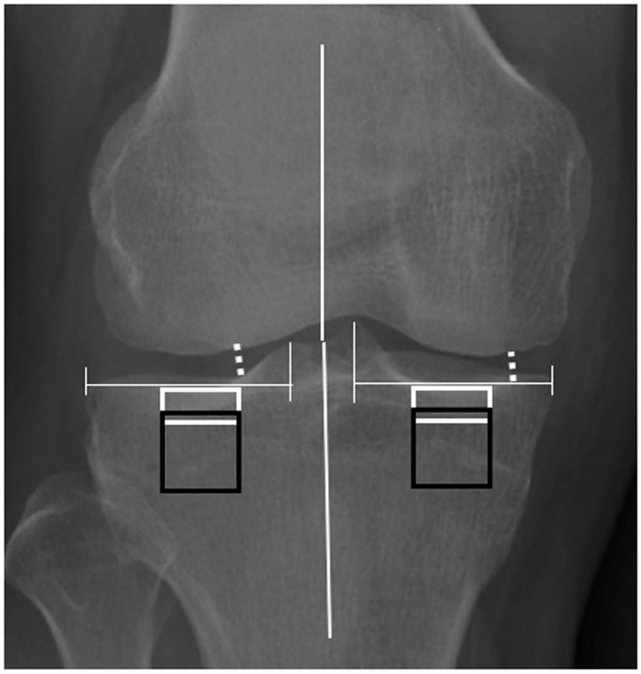

Figure 5. Schematic figure of placement ROIs. Two subchondral bone ROIs (93 × 40 pixels, white rectangles) were placed under the cartilage-bone interface in the middle part of medial and lateral condyles of the tibia. Two trabecular bone ROIs (93 × 93 pixels, black rectangles) were placed below and parallel to the subchondral bone ROIs of the tibia. Minimum JSWs (white dotted line) were measured from the narrowest point of the joint from both the medial and the lateral sides. Anatomical angles were medially measured from the intersection of a line from the center of the head of femur to the center of the tibial spines, and a second line from the center of the tibia to the center of the tibial spines.

horizontally, then combined into one matrix. A final Laplacian-based image was obtained after an unprocessed ROI was multiplied with square root of Laplacian matrix and further expanded to a full dynamic range. The entropy of image (E_{Lap}) was used to present the randomness of grayscale values in Laplacian-based image[7,14,15] calculated with following equation 1:

$$E_{Lap} = -\sum_i P_i \log 2\ P_i, \quad (1)$$

where E_{Lap} is the entropy of a statistical textural characteristic of randomness, and P_i is the normalized grayscale value i in the image.

Local binary patterns (LBP)-based methods. LBP, a 2D texture spectrum model on pixel level in grayscale, have been a powerful feature for texture classification in computer vision field[25,26]. It encodes the relative strength of the center pixel and its surrounding pixels, which represents eight elements. Each of those has one of two possible values (0, 1) obtained from a neighborhood of 3 × 3 pixels. The center pixel is set up as threshold and compares to 8-neighborhood pixel. LBP-based methods were used to evaluate the randomness of local binary patterns of the images and the dissimilarities in the orientation of adjacent local binary patterns as described elsewhere in previous studies[10,15,27]. Briefly, the bone and non-bone areas of the image was determined using Otsu method and LBPs were calculated from these regions. The number of possible patterns was reduced by determining the main orientation of each pattern. The orientation angles (0°, 45°, 90°, and 135°) were computed for the patterns consisting of two to five consecutive markers. Rest of the patterns were considered as non-uniform. The entropy of the grouped patterns (E_{LBP}) determined with equation (1) was used to present the randomness of the patterns in an image.

Homogeneity index (HI) for orientation of local patterns. HI, a spatial distribution of gray-level co-occurrence matrix in an image, evaluates the variations in neighboring pattern orientations along the defined direction. The co-occurrence matrices of local pattern angles were computed at 0°, 45°, 90°, and 135° directions within one pixel's distance. HI-derived from the gray-level co-occurrence matrix was calculated perpendicular (HI_{Perp}, combination of 45° and 90°) and parallel (HI_{Paral}, combination of 0° and 135°) to the trabecular main orientation[15]. The mean of HI (HI_{Mean}) was the sum of the four possible directions calculated from the co-occurrence matrices.

Fractal signature analysis (FSA). FSA is used to quantify degree and content of the roughness of bone texture structure in an image as previously described[10,15,28,29]. In practice, the original image is firstly dilated and eroded in vertically and horizontally with a structuring element that is rod-shaped and one-pixel-wide[15,18], and whose length varied from 2 to 4 pixels. The volume measured between the dilated and eroded image and the structuring

element length were used to calculate surface area, which was made in log-log plot and then together with structuring element length, were used to estimate FD by using a regression line to points. When the structuring element is pointing in vertical direction, FD of horizontal structures (FD_{Hor}) is produced, similarly, the horizontal direction produces FD of vertical structure (FD_{Ver})[15,18,30].

Statistical analysis. Statistical analyses were performed using IBM SPSS statistics 24 software. The differences of structure-related parameters between controls and KBD patients, and various KBD subgroups were evaluated with non-parametric independent Mann-Whitney U/Kruskal Wallis H sample test. *P* value of <0.05 was considered as statistical significance.

Statistics and biometry. Jukka Hirvasniemi kindly provided statistical advice for this manuscript.

Informed consent. Written informed consent was obtained from all subjects (patients) in this study.

Ethical approval. Institutional Review Board approval was obtained from "The first Affiliated Hospital of Xi´an Jiaotong University Ethics Committee".

Study subjects or cohorts overlap. Study subjects or cohorts have not been previously reported.

Methodology. Retrospective, cross sectional study, performed at one institution. All methods were carried out in accordance with relevant guidelines and regulations.

Data Availability

The original, raw data and quantitative data considering the basic information, medJSW, latJSW, tibia width and anatomical angle of the knees, bone structural parameters (E_{Lap}, E_{LBP}, HI, FD) from subchondral and trabecular bone of the studied subjects used to support the findings of this study are available from corresponding author upon reasonable request. The images for patient's clinical and radiological findings as well as the placement of ROIs used to support the findings of this study are available from corresponding author upon request.

References

1. Guo, X. Diagnostic, clinical and radiological characteristics of Kashin-Beck disease in Shaanxi Province, PR China. *Int Orthop.* **25**, 147–150, https://doi.org/10.1007/s002640100248 (2001).
2. Kraus, V. B. Rare Osteoarthritis: Ochronosis and Kashin-Beck Disease. In: *Rheumatology, 6th edition*, Eds M. C. Hochberg, A. J. Silman, J. S. Smolen, M. E. Weinblatt & M. H. Weisman (Mosby Elsevier, Philadelphia). Chapter 185, 1536–1540 (2014).
3. Malaisse, F. & Mathieu, F. Big bone disease. A multidisciplinary approach of KBD in Tibet autonomous region (P.R. China). Les *Presses agronomiques de Gembloux*, A.S.B.L. 70–78 (2008).
4. Yu, F. F. *et al*. Evaluation of the sensitivity and specificity of the new clinical diagnostic and classification criteria for Kashin-Beck disease, an endemic osteoarthritis, in China. *Biomed Environ Sci.* **30**, 150–155, https://doi.org/10.3967/bes2017.021 (2017).
5. Hinsenkamp, M. *et al*. The anatomical distribution of radiological abnormalities in Kashin-Beck disease in Tibet. *Int Orthop.* **25**, 142–146, https://doi.org/10.1007/s002640100236 (2001).
6. Wang, Y., Yang, Z., Gilula, L. A. & Zhu, C. Kashin-Beck disease: radiographic appearance in the hands and wrists. *Radiology.* **201**, 265–270, https://doi.org/10.1148/radiology.201.1.8816556 (1996).
7. Hirvasniemi, J. *et al*. Quantification of differences in bone texture from plain radiographs in knees with and without osteoarthritis. *Osteoarthritis Cartilage.* **22**, 1724–1731, https://doi.org/10.1016/j.joca.2014.06.021 (2014).
8. Bacchetta, J. *et al*. Assessment of bone microarchitecture in chronic kidney disease: a comparison of 2D bone texture analysis and high-resolution peripheral quantitative computed tomography at the radius and tibia. *Calcif Tissue Int.* **87**, 385–391, https://doi.org/10.1007/s00223-010-9402-z (2010).
9. Guggenbuhl, P., Bodic, F., Hamel, L., Basle, M. F. & Chappard, D. Texture analysis of X-ray radiographs of iliac bone is correlated with bone micro-CT. *Osteoporos Int.* **17**, 447–454, https://doi.org/10.1007/s00198-005-0007-8 (2006).
10. Hirvasniemi, J. *et al*. Correlation of subchondral bone density and structure from plain radiographs with micro computed tomography *ex vivo*. *Ann Biomed Eng.* **44**, 1698–1709, https://doi.org/10.1007/s10439-015-1452-y (2016).
11. Le Corroller, T. *et al*. Bone texture analysis is correlated with three-dimensional microarchitecture and mechanical properties of trabecular bone in osteoporotic femurs. *J Bone Miner Metab.* **31**, 82–88, https://doi.org/10.1007/s00774-012-0375-z (2013).
12. Luo, G. *et al*. Relationship between plain radiographic patterns and three- dimensional trabecular architecture in the human calcaneus. *Osteoporos Int.* **9**, 339–345, https://doi.org/10.1007/s001980050156 (1999).
13. Ollivier, M. *et al*. Radiographic bone texture analysis is correlated with 3D microarchitecture in the femoral head, and improves the estimation of the femoral neck fracture risk when combined with bone mineral density. *Eur J Radiol.* **82**, 1494–1498, https://doi.org/10.1016/j.ejrad.2013.04.042 (2013).
14. Thevenot, J. *et al*. Assessment of risk of femoral neck fracture with radiographic texture parameters: a retrospective study. *Radiology.* **272**, 184–191, https://doi.org/10.1148/radiol.14131390 (2014).
15. Hirvasniemi, J. *et al*. Differences in tibial subchondral bone structure evaluated using plain radiographs between knees with and without cartilage damage or bone marrow lesions - the Oulu Knee Osteoarthritis study. *Eur Radiol*. https://doi.org/10.1007/s00330-017-4826-8 (2017).
16. Thevenot, J. *et al*. Local binary patterns to evaluate trabecular bone structure from micro-CT data: application to studies of human osteoarthritis. In: *Lourdes Agapito, Michael M. Carsten Rother (Eds.), Computer Vision-ECCV 2014 Woekshops. Lecture Notes in Computer Science*, Vol. 8926 63–79, https://doi.org/10.1007/978-3-319-16181-5.5 (2015).
17. Lynch, J. A., Hawkes, D. J. & Buckland-Wright, J. C. A robust and accurate method for calculating the fractal signature of texture in macroradiographs of osteoarthritic knees. *Med Inform (Lond).* **16**, 241–251, https://doi.org/10.3109/14639239109012130 (1991).
18. Lynch, J. A., Hawkes, D. J. & Buckland-Wright, J. C. Analysis of texture in macroradiographs of osteoarthritic knees using the fractal signature. *Phys Med Biol.* **36**, 709–722, https://doi.org/10.1088/0031-9155/36/6/001 (1991).
19. Kraus, V. B. *et al*. Trabecular morphometry by fractal signature analysis is a novel marker of osteoarthritis progression. *Arthritis Rheum.* **60**, 3711–3722, https://doi.org/10.1002/art.25012 (2009).
20. Podsiadlo, P., Dahl, L., Englund, M., Lohmander, L. S. & Stachowiak, G. W. Differences in trabecular bone texture between knees with and without radiographic osteoarthritis detected by fractal methods. *Osteoarthritis Cartilage.* **16**, 323–329, https://doi.org/10.1016/j.joca.2007.07.010 (2008).

21. Wolski, M., Podsiadlo, P., Stachowiak, G. W., Lohmander, L. S. & Englund, M. Differences in trabecular bone texture between knees with and without radiographic osteoarthritis detected by directional fractal signature method. *Osteoarthritis Cartilage.* **18**, 684–690, https://doi.org/10.1016/j.joca.2010.01.002 (2010).
22. Wolski, M., Podsiadlo, P. & Stachowiak, G. W. Directional fractal signature methods for trabecular bone texture in hand radiographs: data from the Osteoarthritis Initiative. *Med Phys.* **41**, 081914, https://doi.org/10.1118/1.4890101 (2014).
23. Wolski, M. *et al*. Trabecular bone texture detected by plain radiography and variance orientation transform method is different between knees with and without cartilage defects. *J Orthop Res.* **29**, 1161–1167, https://doi.org/10.1002/jor.21396 (2011).
24. Kraus, V. B., Vail, T. P., Worrell, T. & McDaniel, G. A comparative assessment of alignment angle of the knee by radiographic and physical examination methods. *Arthritis Rheum.* **52**, 1730–1735, https://doi.org/10.1002/art.21100 (2005).
25. Ojala, T., Pietikäinen, M. & Harwood, D. Comparative study of texture measures with classification based on feature distributions. *Pattern Recognition.* **29**, 51–59, https://doi.org/10.1016/0031-3203(95)00067-4 (1996).
26. Wang, L. & He, D. C. Texture classification using texture spectrum. *Pattern Recognition.* **23**, 905–910, https://doi.org/10.1016/0031-3203(90)90135-8 (1990).
27. Hirvasniemi, J. *et al*. Association between radiography-based subchondral bone structure and MRI-based cartilage composition in postmenopausal women with mild osteoarthritis. *Osteoarthritis Cartilage*. https://doi.org/10.1016/j.joca.2017.09.008 (2017).
28. Buckland-Wright, J. C., Lynch, J. A. & Macfarlane, D. G. Fractal signature analysis measures cancellous bone organisation in macroradiographs of patients with knee osteoarthritis. *Ann Rheum Dis.* **55**, 749–755, https://doi.org/10.1136/ard.55.10.749 (1996).
29. Pothuaud, L. *et al*. Fractal dimension of trabecular bone projection texture is related to three-dimensional microarchitecture. *J Bone Miner Res.* **15**, 691–699, https://doi.org/10.1359/jbmr.2000.15.4.691 (2000).
30. Caldwell, C. B., Moran, E. L. & Bogoch, E. R. Fractal dimension as a measure of altered trabecular bone in experimental inflammatory arthritis. *J Bone Miner Res.* **13**, 978–985, https://doi.org/10.1359/jbmr.1998.13.6.978 (1998).

Acknowledgements

The authors express their appreciation for the support of Faculty of Medicine, Umeå University, Academy of Finland (grant nos 268378 and 308165) and Key international cooperation research project of the National Natural Science Foundation of China (grant no. 8162010826). The funding sources had no role in the study design, data collection, analysis and interpretation, drafting of manuscript, or in the decision to submit the manuscript for the publication.

Author Contributions

W.R. Li and X. Guo collected the studied materials. C.J. Qu, M.J. Lammi, J. Hirvasniemi and S. Saarakkala designed the study. J. Hirvasniemi measured the bone texture. S. Saarakkala and M.J. Lammi provided the supervision of the data analysis and manuscript. C.J. Qu and J. Hirvasniemi analyzed the results. C.J. Qu wrote the paper. All authors were involved in revising the manuscript critically for important intellectual content and approved the final version to be submitted.

Additional Information

Supplementary information accompanies this paper at https://doi.org/10.1038/s41598-018-35552-8.

Competing Interests: The authors declare no competing interests.

Publisher's note: Springer Nature remains neutral with regard to jurisdictional claims in published maps and institutional affiliations.